JOURNAL OF GEOPHYSICAL RESEARCH, VOL. 92, NO. A13, PAGES 15,217–15,224, DECEMBER 30, 1987

Plasma Wave Measurements in the Magnetosphere of Uranus

F. L. Scarf,[1] D. A. Gurnett,[2] W. S. Kurth,[2] F. V. Coroniti,[1]
C. F. Kennel,[1] and R. L. Poynter[3]

As Voyager 2 traversed the magnetosphere of Uranus, the plasma wave instrument detected very significant phenomena related to local wave-particle interactions, radio emissions, and dust impacts. Here we consider the region between the inbound and outbound bow shock traversals (covering a distance of more than 250 R_U), and we demonstrate that intense plasma wave activity developed only in the inner magnetosphere ($r < 12\ R_U$); this result is similar to that found at Saturn, but it is in marked contrast with the Jupiter case, where very strong wave activity was detected out to distances of 250 R_J. The Uranus plasma wave observations in the inner magnetosphere are compared with corresponding results from the Jupiter and Saturn encounters, and it is shown that the Uranus wave measurements are unique in several significant ways. These new aspects include (1) the detection of a marked inbound-outbound asymmetry and (2) the detection of whistler mode waves that yield the strongest wave-particle interactions found in outer planet magnetospheres.

1. Introduction

In the initial summary reports on the Voyager 2 plasma wave observations at Uranus, *Gurnett et al.* [1986], *Kurth et al.* [1986], and *Scarf et al.* [1986] demonstrated that strong electromagnetic and electrostatic plasma turbulence, low-frequency radio emissions, and dust impacts were all readily detected during the encounter. Here we review the Uranus wave measurements in the context of a discussion of magnetospheric dynamics, and we try to identify features that are familiar for outer planet magnetospheres, and those that appear to be unique.

Section 2 contains a description of the operation of the plasma wave instrument at Uranus, followed by a brief overview of the encounter highlights covering the traversal from bow shock to bow shock. In section 3 we reexamine the inner magnetosphere wave measurements using the latest information on the planetary magnetic field, and in section 4 we compare these Uranus observations with corresponding results from Jupiter and Saturn. Several aspects of the Uranus wave measurements appear to be quite unusual in terms of expectations based on the Jupiter-Saturn data sets. We call attention to specific phenomena involving the absence of strong low-frequency plasma turbulence (lower hybrid resonance emissions and electromagnetic hiss) and the very great asymmetry between inbound and outbound wave amplitudes; it is likely that magnetic latitude variations can account for this asymmetry, but the possibility of temporal changes, such as substorm effects, cannot be dismissed.

The companion papers in this issue contain more detailed studies that are focused on specific phenomena; *Gurnett et al.* [this issue] analyze the dust impacts detected at the ring plane crossing, *Kurth et al.* [this issue] discuss electrostatic waves in the magnetosphere of Uranus, and *Coroniti et al.* [this issue] present a quantitative analysis of the interactions involving the whistler mode emissions and the energetic radiation belt electrons.

[1] TRW Space and Technology Group, Redondo Beach, California.
[2] University of Iowa, Iowa City.
[3] Jet Propulsion Laboratory, California Institute of Technology, Pasadena.

Paper number 7A9019.
0148-0227/87/007A-9019$05.00

2. Encounter Overview

The Voyager plasma wave instrument uses a balanced electric dipole antenna with a 7-m effective length. During planetary encounters the signals are continuously processed with a 16-channel analyzer that yields a spectrum covering the range 10 Hz to 56 kHz, with a sampling rate of one scan per 4 s. In addition, during certain very brief intervals the output of a wideband receiver is sampled 28,800 times per second, and the waveform records are stored on the tape recorder for subsequent transmission to Earth. The initial format for these high-rate waveform measurements involved 48-s-long intervals [*Scarf and Gurnett*, 1979], and this format was used for both the Jupiter and Saturn encounters [*Scarf et al.*, 1981, 1983]. However, because of the great distance between Earth and Uranus and the associated very low telemetry rates available during tape recorder playback, for the 1986 encounter there were few opportunities to record full 48-s-long intervals (or "frames"). Thus a new 10-s-long frame was developed for use at Uranus, and the measurement interval was placed within the normal 48-s sequence during specific times when known periodic spacecraft interference signals would be absent.

The Voyager plasma wave measurement capabilities are graphically indicated on the left side of Figure 1, and the right-hand side shows some of the nominal characteristic frequencies in the solar wind plasma as a function of distance from the Sun. Here f_p^+ and f_p^- represent the proton and electron plasma frequencies, and f_c^- is the electron cyclotron frequency (f_p^- (in kilohertz) $= 9(N)^{1/2}$, where N is the electron density in particles per cubic centimeter; $f_p^+ = f_p^-/43$; f_c^- (in hertz) $= 28B$, where B is the interplanetary magnetic field strength in nanoteslas). It can be seen that as R increases, f_p^- steadily declines, and thus by the time that Voyager approached Uranus in January 1986, the window for detecting planetary radio emissions had expanded downward into the middle of the plasma wave frequency range. In fact, the first plasma wave indication of a planetary encounter involved detection of strong radio emissions on January 19, 1986, when Voyager 2 was at a distance of 270 R_U [*Gurnett et al.*, 1986]; these waves appeared in the 31- and 56-kHz channels, and corresponding signals were observed throughout the encounter in these channels and in the 18-kHz channel.

During the traversal of the planetary foreshock, electron plasma oscillations were briefly detected on January 23 (between 0530 and 1300), and they were again detected fairly continuously starting at 0300 on January 24. The bow shock itself was crossed at 0730 on January 24; Figure 2 contains a

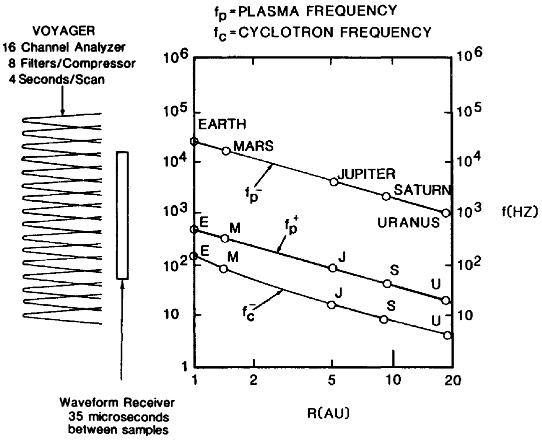

Fig. 1. The variation in characteristic interplanetary plasma wave frequencies with distance from the Sun. The drawings on the left side show the measurement capabilities of the Voyager 2 plasma wave instrument. Each filter has a bandwidth that is 15% of the center frequency.

calibrated 12-channel plasma wave amplitude plot for this initial inbound crossing and similar information for one of the final bow shock traversals (the 178- and 311-Hz data are omitted from Figure 2 because these channels were strongly contaminated by interference at this time). The bottom panel in the figure, adapted from a drawing by *Ness et al.* [1986], shows the magnetic field profile for the entire encounter, and all of the bow shock traversals are marked here.

In terms of the plasma wave observations the first inbound crossing was unusually irregular and diffuse, and the magnetometer and plasma probe also detected considerable structure in the postshock region [*Bagenal et al.*, 1987]. Figure 2 shows that the inbound crossing detected on January 28, 1986, had the normal thin shock behavior that appears to be characteristic for outer planet bow shock crossings [*Scarf et al.*, 1981, 1983], and we speculate that the unusual appearance of the January 24 crossing may have involved a response to changes in the magnitude of the solar wind pressure.

The upper panel of Figure 3 contains a summary of the wave measurements within the magnetosphere, and the lower panel (adapted from Figure 1 of *Bridge et al.* [1986]) shows the profile of the 10-eV to 1-keV ion flux measured simultaneously by the Voyager 2 plasma probe. This drawing clearly demonstrates that at Uranus the intense wave activity was confined to a very limited region centered about closest approach. The local plasma waves (those with f below or slightly above the electron cyclotron frequency) were detected only when Voyager was within 10 R_U, and the strong wave activity was generally correlated with the detection of high fluxes of low-energy protons.

The Saturn encounters were similar in the sense that the Voyager wave instruments detected the most intense activity within about 10 R_S (see Figure 5 of *Scarf et al.* [1983]), but at Jupiter the situation was very different. This distinction is readily apparent in any of the Jupiter summary plots (see, for instance, Plate 1 of *Scarf et al.* [1981]), since the wave emissions designated as trapped continuum radiation were extremely intense and they were readily detected out to distances of 70 R_J on the inbound passes and 240 R_J as the Voyager spacecraft departed from Jupiter. In the Jovian magnetosphere the strongest of these signals were near the lower-frequency cutoff, and they were recently identified as Z mode emissions

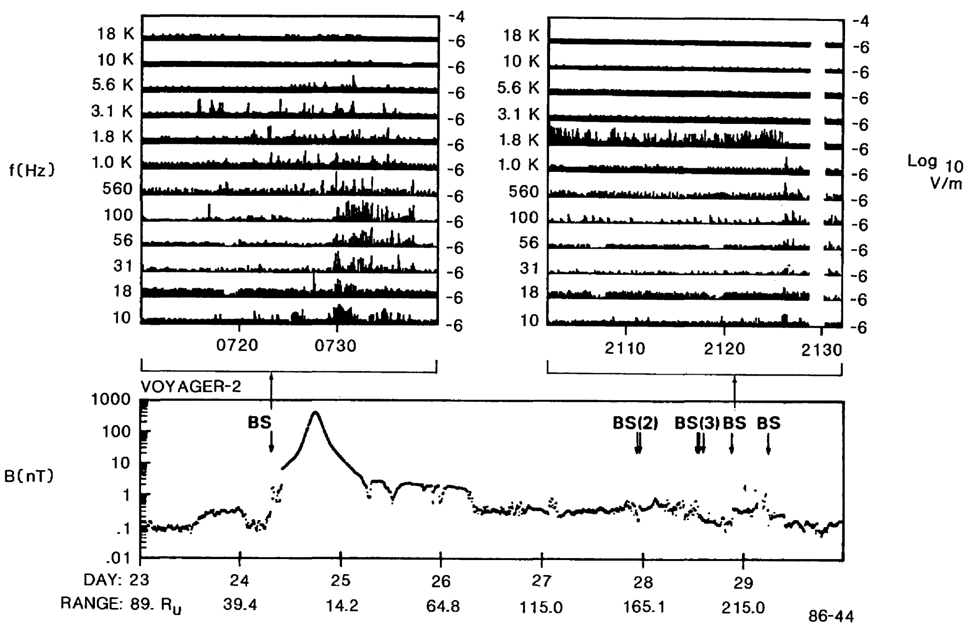

Fig. 2. Wave measurements at Uranus bow shock crossings. The bottom panel shows the magnetic field magnitude, as presented by *Ness et al.* [1986], and the BS label represents a shock crossing. The (unaveraged) wave amplitude profiles for the initial and final inbound crossings are displayed at the top.

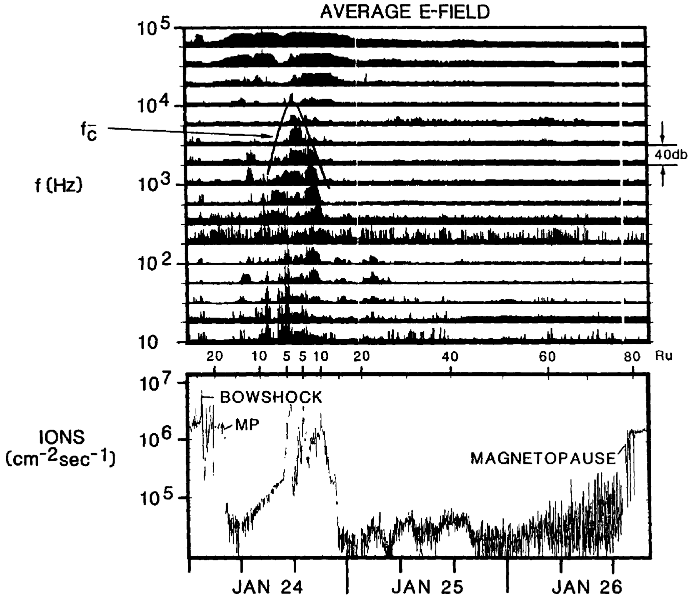

Fig. 3. The upper panel contains 16-channel *E* field averages for the entire traversal of the Uranus magnetosphere, and the lower drawing, adapted from *Bridge et al.* [1986], shows the variation in ion flux measured by the Voyager 2 plasma probe. The profile of f_c^-, the electron cyclotron frequency, is obtained from the Voyager 2 magnetometer data. The sporadic noise in the 178-kHz channel represents interference from another Voyager science instrument.

[*Kennel et al.*, 1987; *Moses et al.*, 1987]. However, at Jupiter, even the conventional electromagnetic continuum waves with frequencies well above the lower cutoff were so strong that they were detectable whenever the spacecraft were located in regions with low plasma density.

The absence of comparable trapped continuum radiation at Uranus is especially significant for the outbound pass, where the measurements from the plasma probe, the low-energy charged particle instrument, and the magnetometer were used to identify a number of plasma sheet and current sheet crossings [*Bridge et al.*, 1986; *Krimigis et al.*, 1986; *Ness et al.*, 1986]. Since the trapped continuum wave levels were too low to be easily detected by the plasma wave instrument (although a very weak 1.78-kHz emission that may have been continuum radiation was barely detected just within the inbound traversal of the magnetopause, as noted by *Gurnett et al.* [1986]), we cannot provide absolute information on plasma density variations in the Uranus tail.

3. THE INNER MAGNETOSPHERE

Gurnett et al. [1986] first discussed the plasma wave observations in the inner magnetosphere of Uranus in terms of a 16-channel plot of peak and average wave amplitudes for the interval 1500–2130 on January 24, 1986. Figure 4 has a 16-channel plot that covers almost the same time interval and has the same amplitude scale, but here we display only the *E* field averages (over 48 s), and we also plot our best estimate of the electron plasma frequency profile (see *Kurth et al.* [this issue] for a discussion of the basis for a density model that is essentially the same). In both cases the f_c^- curve is derived from *B* field values measured by the Voyager magnetometer team, while the magnetic field parameters shown in the upper panel of Figure 4 are based on use of the Q_3 model [*Connerney et al.*, this issue].

Figure 4 shows low-frequency radio emissions (waves with f greater than the local plasma frequency), electron gyrofrequency harmonics (waves with f slightly greater than the electron cyclotron frequency), and strong wave activity for f less than f_c^-. In order to assess the significance of these results, it is useful to note that Voyager 2 traversed three special locations during the middle part of its journey through the inner magnetosphere: (1) the ring plane (or spin equatorial plane) was crossed at 1715:26 UT, as marked at the bottom of Figure 4; (2) closest approach to Uranus ($r = 4.19$ R_U) occurred at 1800 UT; and (3) closest approach to the magnetic equator (magnetic latitude is 6.45°) occurred near 1925 UT. Fortunately, we were able to record three 48-s-long wideband frames at the ring plane crossing and one at closest approach. We also were able to record a number of 10-s frames near 1925, and color-coded frequency-time spectrograms made up from the wideband data are shown in Plate 1. The analysis of the Uranus plasma wave data in the inner magnetosphere is based on study of the 16-channel measurements and the wideband observations.

Gurnett et al. [1986] identified the ring plane crossing signals as impulses associated with dust impacts on the Voyager spacecraft, and this interpretation is strongly supported by inspection of the waveform data. The frequency-time diagram for the equator crossing interval is displayed in the top panel of Plate 1, and these waveform measurements show the typical broadbanded but featureless spectra that appear when the spacecraft is bombarded by a high flux of dust particles (this spectrogram closely resembles the corresponding one for the Saturn ring plane crossing, as shown in Plate 2 of *Scarf et al* [1983]). The audio recordings made up from these data clearly confirm the dust impact explanation (the sounds resemble those of hail impacts on the roof of an automobile), and a detailed analysis of the Uranus dust ring characteristics is contained in the paper by *Gurnett et al.* [this issue].

The electron gyrofrequency harmonics or Bernstein modes

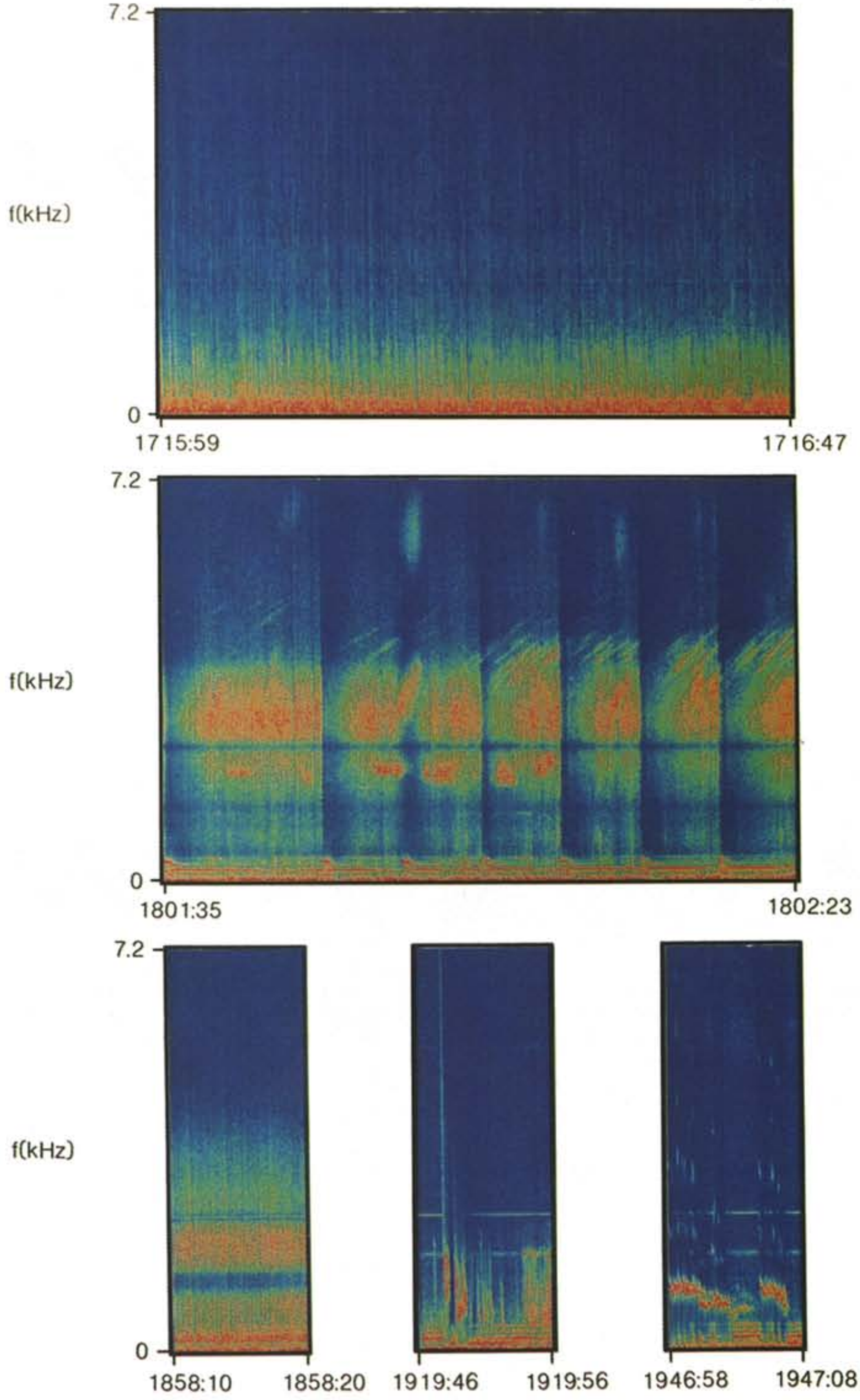

Plate 1. Top: Frequency-time (f-t) diagram showing a broadband wave spectrum of the type detected when Voyager is bombarded by a high flux of dust particles. These signals were detected as Voyager crossed the Uranus ring plane. Center: Closest approach f-t diagram showing characteristic rising tones of whistler mode chorus. When comparing these wave measurements with the 16-channel data of Figure 4 it should be kept in mind that the f-t diagram utilizes a linear frequency scale. Moreover, the automatic gain control amplifier in the waveform channel yields a display that shows only the strongest plasma wave signals. Bottom: Wave spectra detected as Voyager approached the minimum magnetic latitude region (at about 1925 UT) and moved on toward higher magnetic latitudes. We interpret the signals in the left- and right-hand panels as whistler mode emission, but clearly we detected a great asymmetry in wave spectra from inbound to outbound.

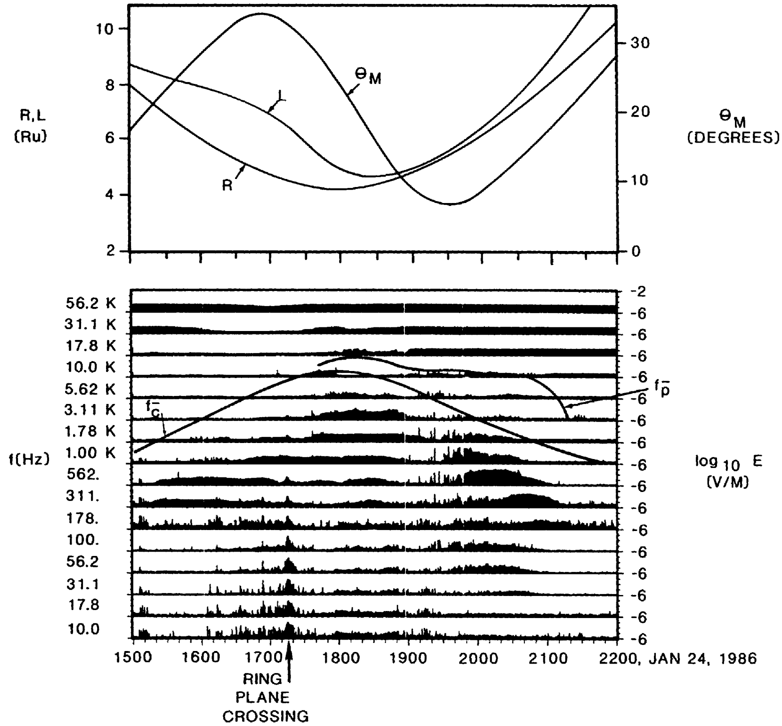

Fig. 4. Plasma wave amplitude measurements and trajectory data for the inner magnetosphere traversal. The wave amplitudes are 48-s averages, and the magnetic field parameters (L values and magnetic latitude) are associated with the Q_3 model [*Connerney et al.*]. The frequency scales used for the plots of the characteristic frequencies here and in Figure 3 are given by the channel baselines. It should be noted that the comparable figures published by *Gurnett et al.* [1986] showed peaks and not averages; the two sets of figures also differ because here we have removed some additional noise bursts associated with firing of the Voyager thrusters.

were discussed in detail by *Kurth et al.* [this issue], and we confine further attention here to characteristics of the Uranus waves with $f < f_c^-$. Figure 4 shows a band of enhanced wave activity with f approximately equal to $(0.1\text{–}0.5)f_c^-$, and since our density model yields a high value for the electron plasma frequency, it is natural to interpret this as whistler mode chorus and hiss. However, we note that the density values are based on models with some uncertainty, and it is possible that the electron plasma frequency could be locally depressed. Indeed, at Saturn we found some low values for f_p^-, and in these regions it turned out that the band-pass channel data alone did not provide an unambiguous identification in all cases; inspection of the Saturn wideband data revealed that some smoothly varying emissions with f comparable to $0.2f_c^-$ were narrow-band radio emissions rather than whistler mode signals [*Gurnett et al.*, 1981*a*, *b*; *Scarf et al.*, 1982], and here we turn again to the wideband data to verify the mode identification.

The central panel of Plate 1 shows the frequency-time diagram recorded at closest approach when the electron cyclotron frequency was just above 10 kHz, and we note that the intense (orange-colored) waves have spectral characteristics very similar to those associated with whistler mode hiss and chorus at Earth and at Jupiter [*Scarf et al.*, 1981]. The strongest signals cover the frequency range 2–4 kHz (or $(0.2\text{–}0.4)f_c^-$), and at the top of the band it is clear that the emission consists of a sequence of bursts with rising frequencies; this rising structure is, in fact, the property that leads to the name "chorus" (the associated audio recordings suggest chirps from a flock of birds).

Figure 4 shows that the wave instrument detected a nearly continuous and regular band of signals with $f < 0.5f_c^-$ during the inner magnetosphere traversal, and it can be concluded that these waves with fairly steady amplitudes are all whistler mode emissions. However, the measurements have some very unusual characteristics, and we note specifically that (1) there was a distinct break in the pattern of steady emissions as Voyager traversed the minimum magnetic latitude/Miranda closest approach region (1910 to about 1935) and (2) there was a striking asymmetry in the wave amplitudes detected before and after approach to the minimum magnetic latitude.

One aspect of the inbound-outbound asymmetry is illustrated in Figure 5, where the 562-Hz plasma wave amplitude profile is plotted on an expanded vertical scale. It can be seen that the signals detected near 2000 UT had field strengths approximately 30 times greater than the corresponding signals detected on the same L shell during the inbound pass. This great disparity (which implies a factor of 900 difference in wave power for pitch angle scattering) could simply be associated with the large magnetic latitude difference (note the values at the bottom of Figure 5), but another explanation involving a large-scale magnetospheric temporal variation (e.g., a substorm) is also worthy of consideration (*Mauk et al.* [this issue] noted that some Voyager measurements of energetic particle characteristics were suggestive of substorm injection phenomena).

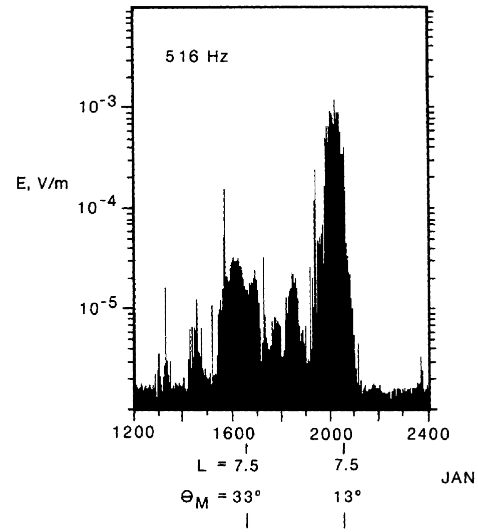

Fig. 5. Expanded amplitude plot showing the inbound-outbound whistler mode asymmetry, which could be related to the change in magnetic latitude or to temporal variations.

The wideband observations associated with the traversal of the minimum magnetic latitude/Miranda closest approach point also reveal a significant asymmetry, as shown in the bottom panel of Plate 1. The display of successive f-t diagrams with expanded frequency scales for the available 10-s frames recorded during the passage through this region shows that they are all quite distinct, with the following characteristics: (1) the 1858 UT spectrum has a strong featureless noise band with $f = 1.9$–2.5 kHz ($=(0.27$–$0.36)f_c^-$), and this can be categorized as whistler mode hiss; (2) the 1919 UT spectrum (recorded in the "whistler gap") shows a large number of impulsive noise bursts of the type usually associated with ion acoustic wave turbulence (as suggested by *Kurth et al.* [this issue]); and (3) the 1946 spectrum shows an intense structured narrow-band emission with f ranging from 500 Hz to 1.2 kHz ($=(0.16$–$0.39)f_c^-$). Thus these waves have frequencies consistent with a whistler mode identification, together with the high intensities and the rapid frequency variations that are usually associated with chorus. However, for the 1946 observations the waves have a falling structure rather than the more common rising structure of normal chorus. We speculate that these relatively unusual dispersion characteristics are associated with the fact that Voyager 2 was not very near the magnetic equator at 1946 UT, and we classify these waves as chorus, with characteristics modified by propagation effects. With this interpretation the bottom panel in Plate 1 shows a transition from moderate levels of whistler mode hiss to ion acoustic waves to very intense levels of whistler mode chorus; *Coroniti et al.* [this issue] show in detail how the intense whistler mode turbulence levels detected during the outbound pass provide extremely rapid pitch angle scattering for electrons with energies of the order of 30–100 keV.

4. Outer Planet Comparisons

The remaining characteristics of the inner magnetosphere wave measurements at Uranus can best be discussed in terms of a direct comparison with the corresponding Voyager 1 and 2 observations at Jupiter and Saturn. Figure 6 contains the comparable displays of the data for five 12-hour periods centered about closest approach (CA) for each encounter. In each channel we use calibrated electric field amplitudes and 48-s averages; all of the individual channel plots cover the same range extending from 1 μV m^{-1} (at the bottom) to 1 mV m^{-1} (at the top).

Since this is the first common scale comparison for Jupiter and Saturn, it is necessary to comment briefly on the upper four panels of Figure 6 before contrasting this with the Uranus data, and we start with the Jupiter encounters. The Voyager 1 drawing on the upper left side shows a relatively quiescent period between 0925 and 1420 UT when the spacecraft penetrated past the inner edge of the Io torus, but when Voyager was within the torus, the plasma wave instrument detected very intense plasma turbulence in every channel with $f < (0.5$–$0.6)f_c^-$. The primary signals in the torus have been identified as whistler mode hiss and chorus, lower hybrid resonance (LHR) emissions, and Doppler-shifted electrostatic ion acoustic waves, while the most intense waves that appear in the quiescent region are essentially only the LHR modes [*Scarf et al.*, 1981; *Barbosa et al.*, 1985].

During its Jupiter encounter, Voyager 2 skimmed along the outer boundary of the Io plasma torus, and the upper right panel in Figure 6 shows that broadbanded turbulence with $f < 0.3f_c^-$ was again detected when the spacecraft was within about 2 hours of its closest approach (the very intense and steady noise that appeared in every channel between 0040 and 0155 on day 191 is an interference signal associated with a long firing of the on-board thrusters; the prominent signals with $f > f_c^-$ are Jupiter radio emissions). The detection of such a broad spectrum of strong whistler mode emissions when both Voyager 1 and 2 were within the Io torus directly implies that the torus dynamics involve very strong pitch angle scattering from a broad population of trapped electrons with energies ranging from suprathermal to relativisitic values.

At Saturn the corresponding wave-particle interactions were found to be much less significant. The central panels in Figure 6 show some fairly intense E field levels for $f < f_c^-$, but as mentioned above, some of these (e.g., the strong Voyager 1 signals in the 5.6- and 10-kHz channels and the intense Voyager 2 waves in the 5.6-, 3.1-, and 1.78-kHz channels) were identified as radio emissions that do not strongly interact with the local particle population. Whistler mode signals were also identified at Saturn, and they can most readily be seen in the Voyager 1 data as the relatively weak waves with f less than or equal to 1 kHz that have peak intensities near the ring plane/magnetic equator crossing. *Scarf et al.* [1983] identified a subset of these as chorus, and they showed that the Saturn whistlers interacted very weakly with the relatively low fluxes of electrons trapped in the Saturn magnetosphere.

The Uranus data display in the bottom panel has a very distinct appearance, in terms of expectations from the previous Voyager encounters. Figure 6 clearly indicates that the most intense outer planet whistler mode signals were actually detected at Uranus, and the comparison drawing also shows that the "break" in the whistler mode emission near 1925 had no real counterpart at Jupiter or Saturn. Moreover, the large inbound-outbound amplitude change for Uranus whistlers appears to be quite unique.

It is of interest to compare quantitatively the wave-particle interactions associated with the whistler mode signals detected in the magnetospheres of Jupiter, Saturn, and Uranus, but this is a complex problem. Even with an unchanged particle distri-

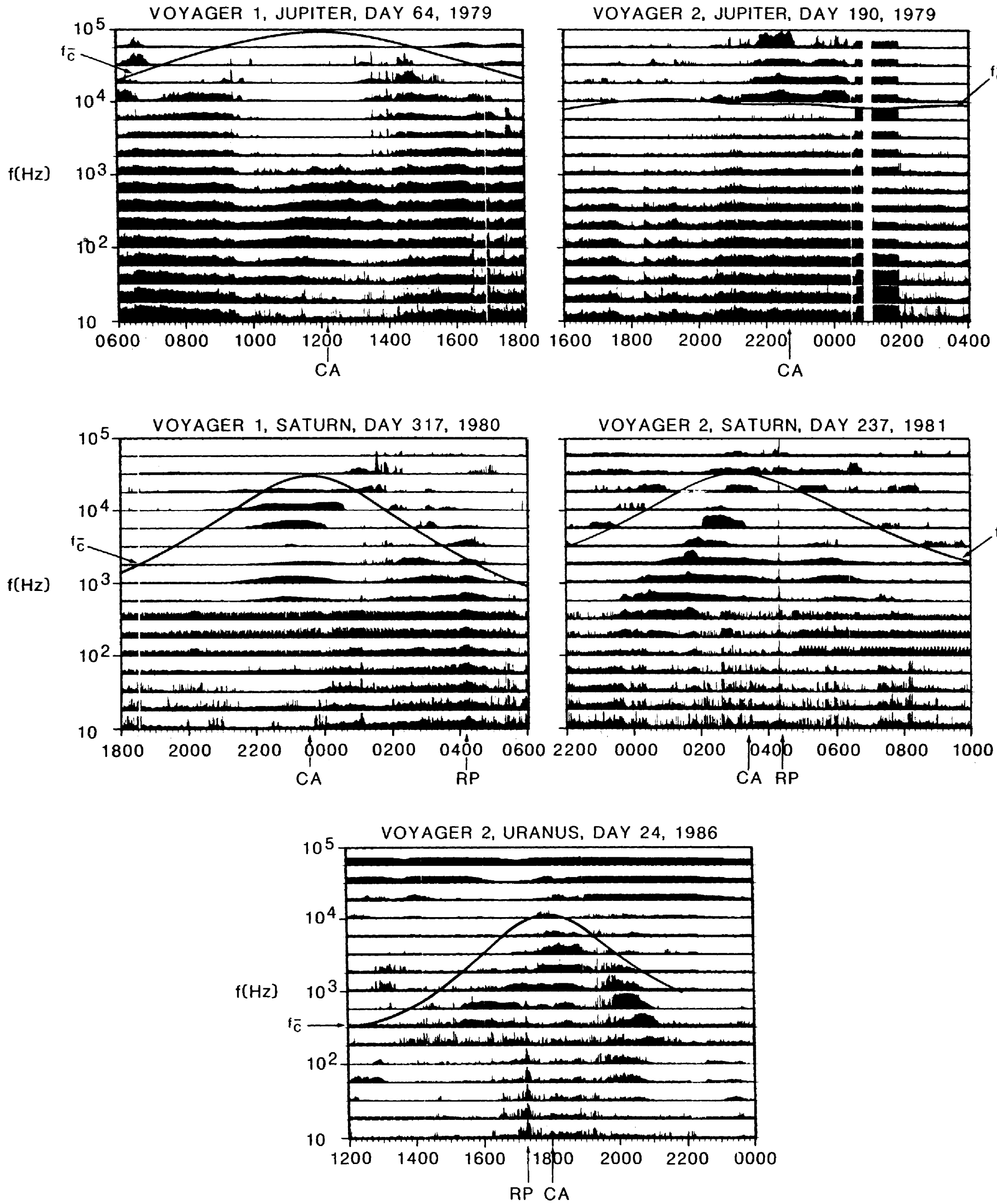

Fig. 6. A comparison of Voyager 1 and 2 plasma wave observations in the inner magnetospheres of Jupiter, Saturn, and Uranus. For each band-pass channel plot the same calibrated amplitude scale is used (1 μV m^{-1} at the bottom to 1 mV m^{-1} at the top), and for each encounter the display covers 12 hours centered about closest approach (labeled CA; for Saturn and Uranus the labels RP designate the ring plane crossings).

bution the effect of a wave with a fixed frequency and E field amplitude will vary strongly as we change the plasma density and field strength, because quantities such as the resonant electron energy and the whistler index of refraction vary with the plasma parameters. However, detailed calculations of pitch angle scattering for these outer planet whistlers have now been completed, and it is possible to compare the results by examining the diffusion rates or the scattering times. At Jupiter, *Thorne* [1983] found a minimum scattering time of 5×10^4 s, and *Scarf et al.* [1984] found that the comparable parameter for Saturn was 3×10^5; *Coroniti et al.* [this issue] note that the minimum scattering time associated with the outbound Uranus passage was only about 10^3 s. Thus the whistler mode wave-particle interactions at Uranus were the strongest detected on the Voyager mission.

Another unusual aspect of the Uranus wave data involves the near absence of detectable signals at low frequencies. The moderate and relatively impulsive wave levels detected in the 56- and 100-Hz channels from 1930 to 2030 UT probably represent detection of lower hybrid resonance emissions, but there is no evidence for whistler mode hiss that could be associated with plasma instabilities induced by anisotropic relativistic electron distributions, in contrast with the situation in the radiation belts of Jupiter and Saturn.

5. DISCUSSION

In terms of the plasma wave observations the Uranus magnetosphere has several unique and perplexing characteristics. The outer planet comparisons show that we detected some of the highest and the lowest plasma wave levels at Uranus. For instance, during the outbound pass we found narrow-band whistler mode signals that must have produced the most intense local wave-particle interactions ever detected by Voyager (see *Coroniti et al.* [this issue] for details), but we also found no evidence for similar strong interactions during the inbound leg, or near closest approach. Moreover, these very strong wave-particle diffusion effects were limited to a narrow range of wave frequencies and electron energies, and there was no evidence of corresponding rapid pitch angle scattering for electrons with relativistic energies.

The more distant Uranus measurements are also unusual in that the Voyager plasma wave instrument was not able to detect trapped continuum radiation or strong wave activity near the outbound plasma sheet crossings. It is possible that some of these unusual wave characteristics are associated with the highly inclined magnetic dipole and with the unique 1986 large-scale configuration of the Uranus magnetosphere that involved near alignment of the rotation axis with the solar wind. For this situation we would expect some characteristics of an open magnetosphere, and perhaps in some way this might lead to an absence of intense trapped continuum radiation. The large tilt of the dipole magnetic field with respect to the planetary spin axis means that for many interplanetary field configurations the planetary and interplanetary fields would periodically be antiparallel; this could yield periodic triggering of substorm activity, perhaps accounting for the inbound-outbound asymmetry.

Acknowledgments. We thank members of the Voyager Magnetometer and Plasma Probe Teams for providing information that was used to compute the electron plasma and cyclotron frequencies, and we are very grateful to Larry Granroth of the University of Iowa for developing the new plot routines that allowed us to use SPAN for remote access of the plasma wave plots. The research at TRW was supported by the National Aeronautics and Space Administration under contracts 954012 and 957805 with the Jet Propulsion Laboratory, while the research at the University of Iowa was supported under contracts 954013 and 957723.

The Editor thanks S. A. Curtis and P. Zarka for their assistance in evaluating this paper.

REFERENCES

Bagenal, F., J. W. Belcher, E. C. Sittler, Jr., and R. P. Lepping, The Uranian bow shock: Voyager 2 inbound observations of a high Mach number shock, *J. Geophys. Res*, *92*, 8603, 1987.

Barbosa, D. D., F. V. Coroniti, W. S. Kurth, and F. L. Scarf, Voyager observations of lower hybrid noise in the Io plasma torus and anomalous plasma heating rates, *Astrophys. J.*, *289*, 392, 1985.

Bridge, H. S., et al., Plasma observations near Uranus: Initial results from Voyager 2, *Science*, *233*, 89, 1986.

Connerney, J. E. P., M. H. Acuña, and N. F. Ness, The magnetic field of Uranus, *J. Geophys. Res.*, this issue.

Coroniti, F. V., W. S. Kurth, F. L. Scarf, S. M. Krimigis, C. F. Kennel, and D. A. Gurnett, Whistler mode emissions in the Uranian radiation belts, *J. Geophys. Res.*, this issue.

Gurnett, D. A., W. S. Kurth, and F. L. Scarf, Plasma waves near Saturn: Initial results from Voyager 1, *Science*, *212*, 235, 1981*a*.

Gurnett, D. A., W. S. Kurth, and F. L. Scarf, Narrowband emissions from Saturn's magnetosphere, *Nature*, *292*, 733, 1981*b*.

Gurnett, D. A., W. S. Kurth, F. L. Scarf, and R. L. Poynter, First plasma wave observations at Uranus, *Science*, *233*, 106, 1986.

Gurnett, D. A., W. S. Kurth, F. L. Scarf, J. A. Burns, J. N. Cuzzi, and E. Grün, Micron-sized particle impacts detected near Uranus by the Voyager 2 plasma wave instrument, *J. Geophys. Res.*, this issue.

Kennel, C. F., R. F. Chen, S. L. Moses, W. S. Kurth, F. V. Coroniti, F. L. Scarf, and F. F. Chen, *Z* mode radiation in Jupiter's magnetosphere, *J. Geophys. Res.*, *92*, 9978, 1987.

Krimigis, S. M., T. P. Armstrong, W. I. Axford, A. F. Cheng, G. Gloeckler, D. C. Hamilton, E. P. Keath, L. J. Lanzerotti, and B. H. Mauk, The magnetosphere of Uranus: Hot plasma and radiation environment, *Science*, *233*, 97, 1986.

Kurth, W. S., D. A. Gurnett, and F. L. Scarf, Sporadic narrow-band radio emissions from Uranus, *J. Geophys. Res.*, *91*, 11,958, 1986.

Kurth, W. S., D. D. Barbosa, D. A. Gurnett, and F. L. Scarf, Electrostatic waves in the magnetosphere of Uranus, *J. Geophys. Res.*, this issue.

Mauk, B. H., S. M. Krimigis, E. P. Keath, A. F. Cheng, T. P. Armstrong, L. J. Lanzerotti, G. Gloecker, and D. C. Hamilton, The hot plasma and radiation environment of the Uranian magnetosphere, *J. Geophys. Res.*, this issue.

Moses, S. L., W. S. Kurth, C. F. Kennel, F. V. Coroniti, and F. L. Scarf, Polarization of low-frequency electromagnetic radiation in the lobes of Jupiter's magnetotail, *J. Geophys. Res.*, *92*, 4701, 1987.

Ness, N. F., M. H. Acuña, K. W. Behannon, L. F. Burlaga, J. E. P. Connerney, R. P. Lepping, and F. M. Neugebauer, Magnetic fields at Uranus, *Science*, *233*, 85, 1986.

Scarf, F. L., and D. A. Gurnett, A plasma wave investigation for the Voyager mission, *Space Sci. Rev.*, *21*, 289, 1979.

Scarf, F. L., D. A. Gurnett, and W. S. Kurth, Measurements of plasma wave spectra in Jupiter's magnetosphere, *J. Geophys. Res.*, *86*, 8181, 1981.

Scarf, F. L., D. A. Gurnett, W. S. Kurth, and R. L. Poynter, Voyager 2 plasma wave observations at Saturn, *Science*, *215*, 587, 1982.

Scarf, F. L., D. A. Gurnett, W. S. Kurth, and R. L. Poynter, Voyager plasma wave measurements at Saturn, *J. Geophys. Res.*, *88*, 8971, 1983.

Scarf, F. L., L. A. Frank, D. A. Gurnett, L. J. Lanzerotti, A. Lazarus, and E. C. Sittler, Jr., Measurements of plasma, plasma waves, and suprathermal charged particles in Saturn's inner magnetosphere, in *Saturn*, edited by T. Gehrels and M. S. Matthews, pp. 318–353, University of Arizona Press, Tucson, 1984.

Scarf, F. L., D. A. Gurnett, W. S. Kurth, and R. L. Poynter, Voyager 2 plasma wave observations at Uranus, *Adv. Space Res.*, *6*, in press, 1986.

Thorne, R. M., Microscopic plasma processes in the Jovian magnetosphere, in *Physics of the Jovian Magnetosphere*, edited by A. J. Dessler, pp. 454–488, Cambridge University Press, New York, 1983.

F. V. Coroniti, C. F. Kennel, and F. L. Scarf, TRW Space and Technology Group, Building R-1, Room 1176, One Space Park, Redondo Beach, CA 90278.

D. A. Gurnett and W. S. Kurth, University of Iowa, Iowa City, IA 52242.

R. L. Poynter, Jet Propulsion Laboratory, California Institute of Technology, 4800 Oak Grove Drive, Pasadena, CA 91109.

(Received March 23, 1987;
revised July 23, 1987;
accepted July 27, 1987.)